Available at
www.ElsevierMathematics.com
POWERED BY SCIENCE DIRECT®

Mathematics and Computers in Simulation 63 (2003) 541–567

MATHEMATICS AND COMPUTERS IN SIMULATION

www.elsevier.com/locate/matcom

Adaptive and statistical expectations in a renewable resource market

Ilaria Foroni [a], Laura Gardini [b,*], J. Barkley Rosser Jr. [c]

[a] *University Bicocca of Milano, Via dell'Ateneo Nuovo 1, 20126 Milano, Italy*
[b] *Institute of Economics, University of Urbino, Via Saffi 2, 61029 Urbino, Italy*
[c] *Department of Economics, James Madison University, Harrisonburg, VA 22807, USA*

Abstract

Rational expectations models have increasingly been replaced by models with various forms of learning. This paper studies the global dynamics of a model of renewable resource markets due to Hommes and Rosser [Macroecon. Dyn. 5 (2001) 180] under adaptive and statistical learning systems. The statistical learning system is seen to generate greater complexity of the structures of the basins of attraction, especially at higher discount rates. An element of particular interest is that bifurcations generating lobes in the basins arise from particular focal points, associated with prefocal sets at infinity on the Poincaré equator in the statistical learning model.

JEL classification: C62; D83; D84; E31; E32; M30

Keywords: Adaptive models; Statistical learning; Fishery models; Complex basins; Global bifurcations

1. Introduction

During the 1970s and 1980s, the rational expectations assumption was considered superior to the previously used adaptive expectations assumption [1]. But more recently it has come to be realized by many of the original advocates of rational expectations that it is more realistic to assume that agents do not initially possess rational expectations but can only move towards that condition through learning [2,3]. Others besides Sargent have come to emphasize that agents are boundedly rational and must learn about market dynamics from experience using various updating mechanisms [4–7].

Boundedly rational learning mechanisms have been shown to allow agents to converge on rational equilibria (RE). However, it is well known that there may be multiple such REs and Evans and Honkapohja [8] show that different learning mechanisms can lead to convergence to different equilibria due to their different transient dynamics. These transient dynamics depend on the global properties of dynamic processes. This becomes especially important when different equilibria differ in their relative optimality.

* Corresponding author. Tel.: +39-0722-305510; fax: +39-0722-305550.
E-mail address: gardini@uniurb.it (L. Gardini).

0378-4754/$30.00 © 2003 IMACS. Published by Elsevier B.V. All rights reserved.
doi:10.1016/S0378-4754(03)00063-6

This paper re-examines a model of renewable resource market dynamics initially studied by Hommes and Rosser [9]. They considered a simple adaptive learning mechanism and showed how agents could learn to believe in a chaotic consistent expectations equilibrium, even with noise and with a smooth underlying model. Following previous work by Bischi and Gardini [10], this paper will compare the adaptive learning mechanism with a fading memory learning mechanism proposed by Lucas [11] and labeled as statistical that has also been studied in [7]. Analysis of the transient dynamics and of the global dynamics follows methods used in [12–14], which have focused on the structure of the basins of attraction and their boundaries. The statistical learning model exhibits a phenomenon only previously observed in an economics model in [15], namely that of lobes in basins of attraction arising from bifurcations at particular focal points, associated with prefocal sets at infinity on the Poincaré equator (whose definition will be given in Section 3).

These results extend earlier ones on learning dynamics in non-linear models in which convergence has been to non-RE attractors or cycles or various forms of complex dynamics [16–22]. They also extend earlier results on models that have regular RE attractors but have complex structures in their basins of attraction, implying potential economic instability [23–25].

Such structures are significant for the model considered by Hommes and Rosser [9], especially when this is applied to the problem of fisheries, which was its main inspiration despite its more general possible application to all renewable resource markets. These complexities of basin structure imply that even in the absence of chaos or other complex dynamics, small perturbations of control parameters can lead to sudden jumps from one basin of attraction to another. In a fishery one could suddenly go from a "good" equilibrium with many fish and low prices to a "bad" equilibrium with few fish and high prices, an outcome resembling that generated by some catastrophe theoretic models of fishery collapse [26,27]. Such phenomena suggest that extra care must be taken in the control of parameters in such situations or that efforts may be needed to change the nature of the learning processes if they tend to generate such outcomes. In the difficult world of actual fisheries such efforts are much easier to recommend than they are to implement.

The plan of the work is as follows. In Section 2, we shall describe the models, one assuming adaptive expectations (Section 2.1), recalling the related dynamic behavior as a function of the rate of discount (δ), and a new one assuming a statistical learning with fading memory (Section 2.2), obtaining a two-dimensional map. Really, we obtain two formulations of this second model. A first one, called map T_α, in which we see that the new model behaves as a standard adaptive one in which the adjustment parameter (α) is replaced by a time-dependent speed of adjustment (α_t). However, this mathematical formulation is quite difficult to study, as described in Section 4. The second is an equivalent, and easier to study, model obtained by a change of coordinate, called map T_W, whose dynamics are studied in Section 3. The asymptotic behaviors, and thus the attracting sets, of the more sophisticated model are already known, while their basins of attractions, that is, the complete knowledge of which points converge towards different attracting sets, are to be determined. This is described in Section 3.1, and we shall see that the learning process has a destabilizing effect with respect to the standard adaptive process. This is mathematically described by a mechanism of formations of particular structures, called "lobes", of one basin inside another basin. These results reformulated in the case of the model T_α, are very interesting from a mathematical point of view, as shown in Section 4, because we can explain bifurcations which otherwise are very difficult to understand, as the bifurcations generating lobes are due to contacts at infinity of arcs issuing from particular focal points, associated with prefocal sets on the Poincaré equator. However, this model becomes more sensitive to parameter changes, that is, a small shock in the state of the system (at any time) may cause a drastic (and worst) change in the asymptotic behavior, as we notice in the conclusions (Section 5).

2. The models

In a cobweb model representing the price dynamics of a perishable-good market, it is assumed that at a given time t the demand function of the consumers depends on the current price p_{t+1} whereas the supply function depends on the price p^{e}_{t+1} expected by producers at the previous time t in which they decided their production. So, if the production delay is taken as the unit time, the market clearing condition becomes $D(p_{t+1}) = S(p^{\mathrm{e}}_{t+1})$. The model of Hommes and Rosser described in [9], and recalled in Appendix A, draws from essentially textbook models of fishery dynamics. The harvesting model is due to Gordon [28] and has costs defined by a linear function of effort and harvest defined by a linear function of effort times the stock of fish. The stock of fish (measured by biomass) depends on a biological growth model due to Schaefer [29] of a simple logistic form. Bioeconomic optimization follows an optimal control formulation due to Clark [30] and is based on sustained yield outcomes with fishers maximizing present value of future harvests.

Given the present value calculation the discount rate used becomes a crucial parameter. As the discount rate rises from zero the supply curve implied by the bioeconomic optimization begins to bend backwards allowing for the possibility of multiple equilibria, an idea first suggested by Copes [31]. An infinite discount rate implies a maximum backward bend of the supply curve and coincides with the open access fishery case initially studied by Gordon [28]. We note that it is not unreasonable to think of the discount rate as a possible control parameter as it may be influenced by market real interest rates.

Hommes and Rosser show this supply curve to be

$$S_\delta(p^{\mathrm{e}}_{t+1}) = f(x^*_\delta(p^{\mathrm{e}}_{t+1})) \tag{1}$$

where $f(x)$ is a logistic function representing the natural growth rate of the population ($x(t)$ denotes the size of the resource population at time t):

$$f(x) = rx\left(1 - \frac{x}{k}\right)$$

the positive constant r represents the *intrinsic growth rate* while the positive constant k is the environmental *carrying capacity* or saturation level, and solving an optimal control problem, assuming that the fishers' objective is the maximization of the total discounted net revenues derived from the exploitation of the resource, the following explicit solution (optimal population level) is obtained (see Appendix A):

$$x^*_\delta(p) = \frac{k}{4}\left\{1 + \frac{c}{pqk} - \frac{\delta}{r} + \sqrt{\left(1 + \frac{c}{pqk} - \frac{\delta}{r}\right)^2 + \frac{8c\delta}{pqkr}}\right\}$$

where $\delta > 0$ denotes the *rate of discount*, q is the *catchability coefficient* (q reflects a combination of technological and biological conditions that relate fishing effort to the harvest of the fish), and c the constant *marginal cost* of fishing effort E. By using the usual linear demand function

$$D(p_t) = A - Bp_t \tag{2}$$

we can express the law of motion for the market clearing price in the following form

$$p_{t+1} = F(p^{\mathrm{e}}_{t+1}), \qquad F(p^{\mathrm{e}}_{t+1}) = D^{-1} \circ S_\delta(p^{\mathrm{e}}_{t+1}) = \frac{A - S_\delta(p^{\mathrm{e}}_{t+1})}{B}. \tag{3}$$

To close the model we must introduce the learning mechanism used by the fishers to foresee the future price. In the next sections, we introduce the adaptive learning and the statistical learning for (3) and then we shall study the dynamics of the models we will obtain in the two different cases. That chaotic dynamics can happen in fisheries with backward-bending supply curves was first noted by Conklin and Kolberg [32], although their model differs somewhat from this one.

2.1. Adaptive expectations

Let us consider first the case in which the producers use a standard adaptive estimation of the expected prices, that is, for $\alpha \in (0, 1)$:

$$p^{\mathrm{e}}_{t+1} = (1-\alpha)p^{\mathrm{e}}_t + \alpha p_t \tag{4}$$

then the map governing the expected price dynamics becomes:

$$p^{\mathrm{e}}_{t+1} = (1-\alpha)p^{\mathrm{e}}_t + \alpha\frac{A - S_\delta(p^{\mathrm{e}}_t)}{B} = g(p^{\mathrm{e}}_t) \tag{5}$$

and it is clear that the sequence of realized prices is obtained from the sequence of expected prices by $p_t = F(p^{\mathrm{e}}_t)$. Thus, the model reduces to a one-dimensional map which, for the sake of simplicity, we rewrite in the following form by using $z = p^{\mathrm{e}}$ and the symbol "′" to denote the unit time advancement operator (i.e. if z is the value of the variable at time t then z' is the value at time $t+1$):

$$z' = g_\alpha(z), \qquad g_\alpha(z) = (1-\alpha)z + \alpha\frac{A - S_\delta(z)}{B} \tag{6}$$

whose dynamics can be easily investigated. Hommes and Rosser [9] observed regimes of bistability of RE, with a backward bending supply curve and reasonable parameter values. Let us briefly recall here the possible dynamics, by using a set of parameter constellations quite close to those used in Hommes and Rosser [9] (which reflect values based on empirical studies used in the work of Clark [30] and the original study of backward-bending supply curves by Cobes [31]), that is

$$A = 5241, \quad r = 0.05, \quad c = 5000, \quad \alpha = 0.5, \quad k = 400,000, \quad q = 0.000014, \quad B = 0.28, \tag{7}$$

assuming δ to be the control-parameter. It is clear that all the dynamics depend on the "shape" of the function $g_\alpha(z)$ (see Fig. 1).

Let us first notice that we shall restrict our analysis to the positive half-line $z > 0$. The complete graph of the function $g_\alpha(z)$ includes a branch in the negative semi-axis, as shown in Fig. 1. However, we can restrict our analysis to the interval $]0, +\infty[$ without loss of generality because this interval is *trapping*, that is, mapped into itself, being $g_\alpha(]0, +\infty[) \subset]0, +\infty[$. This means that any initial condition (i.e. henceforth) with $z > 0$ will have a trajectory completely in the half-line $z > 0$.

It is worth noticing that $g_\alpha(z)$ is unimodal. A unique local minimum value c exists at $c = g_\alpha(c_{-1})$, where $z = c_{-1}$ is the point of local minimum, i.e. critical point of the function $g_\alpha(z)$. Following the notation in [33] (see also [34]), we can say that the map has a "rank-1" critical point at c, that is a point having two coincident (or *merging*) rank-1 pre-images (at c_{-1}). As $g_\alpha(z)$ has no horizontal asymptotes, the local minimum value c separates points of the z-axis having a different number of pre-images. Points belonging to the region $Z_1 =]-\infty, c[$ (see Fig. 1) have only one rank-1 pre-image whereas those belonging to

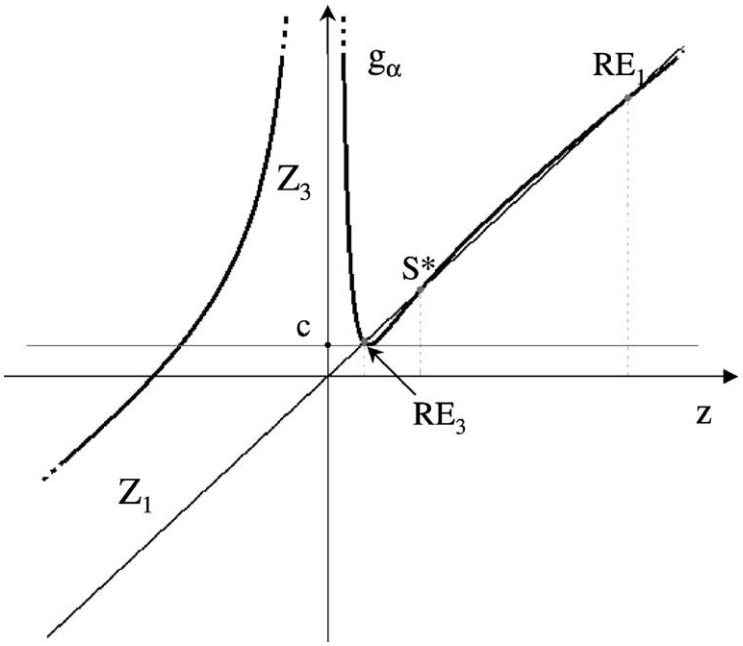

Fig. 1. Complete graph of the function given in (6) with the parameters given in (7) and $\delta = 0.12$.

$Z_3 =]c, +\infty[$ have three distinct pre-images. However, when we look for the rank-1pre-images of a point $z' > 0$, we are only interested in the positive pre-images, which are thus either two distinct ones or none. That is, for any $z' > c$ there are two distinct positive rank-1 pre-images of z' in the positive half-line, while for $0 < z' < c$ there are zero positive rank-1 pre-images. This structure of *the foliation* of the real axis will be used to determine the pre-images of points and thus the basin boundaries.

At low values of δ the map $g_\alpha(z)$ has only one fixed point, RE_3, with a low value of equilibrium price and high fish-quantities, that is, a "good equilibrium" (see Fig. 2). But, as we may expect, as δ increases, local and global bifurcations may occur. At $\delta = \delta_0$ ($\delta_0 \simeq 0.033$), RE_3 becomes unstable via a flip-bifurcation and then a cascade (or Feigenbaum sequence) of period-doubling bifurcations occurs: $\forall n$, a stable 2^n-cycle becomes unstable and gives rise to an attracting 2^{n+1}-cycle. So, as δ increases, the low-level attracting set, say A, becomes more and more complex, and chaotic dynamics occur (see Fig. 3). However, such asymptotic states must always belong to a known interval, which is the interval $[c, c_1]$, where $c_1 = g_\alpha(c)$ is the image of the critical value.

Increasing δ, another equilibrium may appear with a high value of equilibrium price and low fish-quantities, that is, an adverse equilibrium, coexisting (and in competition) with dynamics occurring at low values.

In Fig. 4, we can see that the graph of g_α is close to the main diagonal and when $\delta > \delta_1 \simeq 0.1$ the graph of $g_\alpha(z)$ intersects the bisectrix in two more points, causing the appearance of two new equilibria, one unstable, S^*, and a stable one, called RE_1, as shown in Fig. 5. For $\delta < \delta_1$, the good attractor A is globally stable, while for $\delta > \delta_1$, a new pair of equilibria appear, one of which persists to be stable for δ greater than δ_1. Clearly, the new "bad" equilibrium is in competition with the low-attractor A, and only for suitable initial conditions the dynamics will converge to A. Thus, it is important to know the

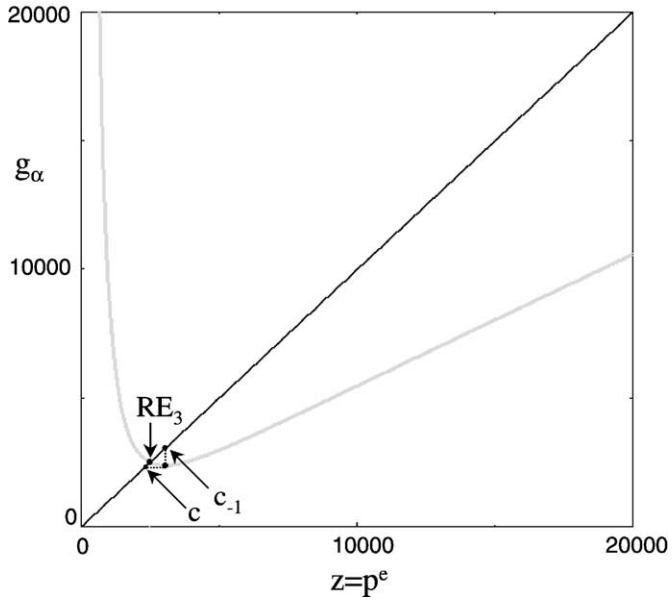

Fig. 2. One rational equilibrium ($\delta = 0.01$).

basins of attraction of the two coexistent attractors. These basins are easily determined, once we know the pre-images of points in the dynamic process.

For $\delta > \delta_1$, the stable set of the unstable equilibrium S^* belongs to the frontier of the two basins of attraction. Let $z = s^*$ be the z-coordinate of the unstable RE, then the two rank-1 pre-images are given by two points, s^*_{-1} and s^*, and as long as we have $s^*_{-1} < c$ (as it occurs in our cases) this point is without

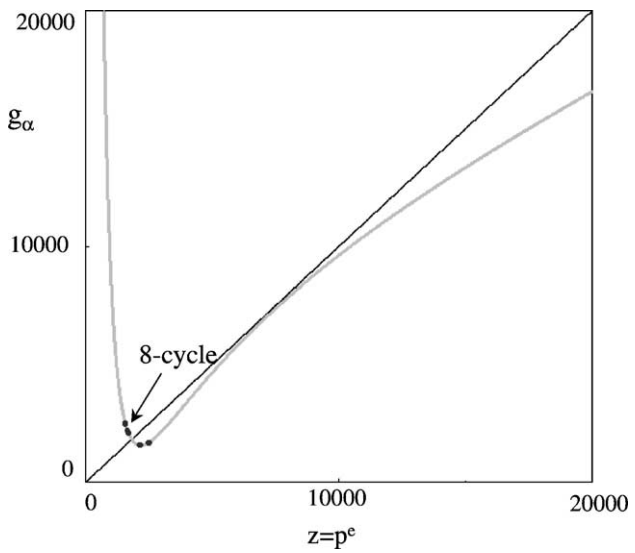

Fig. 3. Graph near the tangent bifurcation ($\delta = 0.1$).

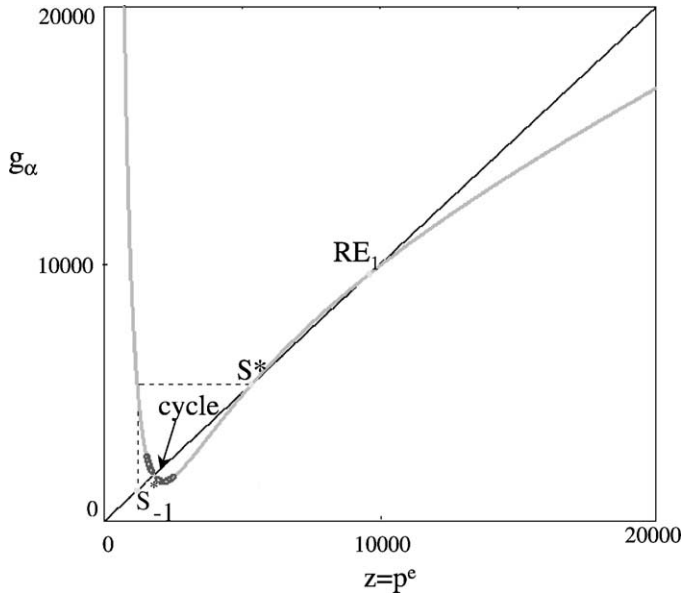

Fig. 4. Three rational equilibria ($\delta = 0.12$)

further pre-images, so we can state (considering the basins only in the half-line $z > 0$) that the basin of attraction of RE_1 is given by the union of two intervals:

$$B(\mathrm{RE}_1) =]0, s^*_{-1}[\cup]s^*, +\infty[.$$

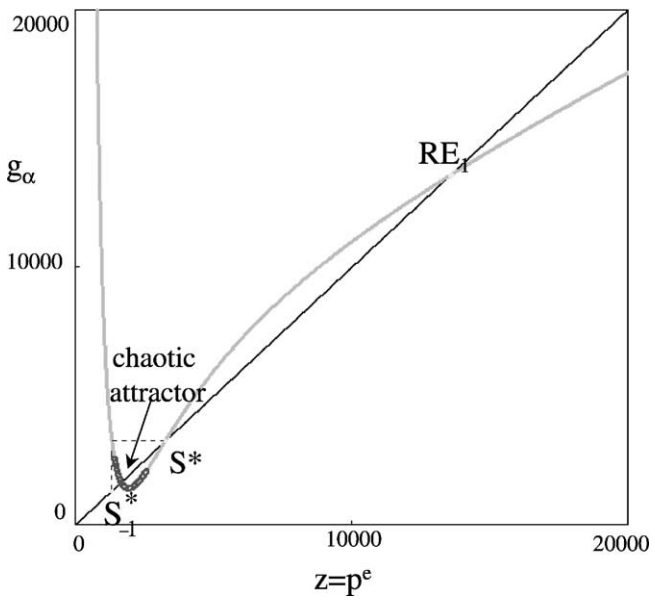

Fig. 5. Low level chaotic attractor ($\delta = 0.5$).

The complementary set is the basin of the absorbing interval $[c, c_1]$ which includes a different attracting set A:

$$B([c, c_1]) =]s^*_{-1}, s^*[.$$

The basin of attraction of the attractor $A \in [c, c_1]$ is the interval $]s^*_{-1}, s^*[$ without at most a denumerable set of points, for example, when A is a cycle we have to exclude from the interval $]s^*_{-1}, s^*[$ the point RE_3 and the points belonging to repelling cycles, as well as their pre-images of any rank. Thus, we can end the analysis of this one-dimensional model with the following proposition:

Proposition 1. *For any $\delta > \delta_1$ there exists a low-level "good" attractor A, coexisting with RE_1 and in competition with it, and the interesting dynamics occur for i.c. in the interval $]s^*_{-1}, s^*[$, the basin $B(A)$ being the interval $]s^*_{-1}, s^*[$ except at most a denumerable set of points.*

2.2. Statistical learning with fading memory

The second learning mechanism we are interested in, called statistical by some authors [7,10,11], is obtained by assuming that at any time t agents compute the expected price for the next time $(t + 1)$ as a weighted arithmetic mean of past realized prices

$$p^{\mathrm{e}}_{t+1} = \sum_{k=0}^{t} a_{tk} p_k$$

and weights

$$a_{tk} \geq 0, \quad k = 0, \ldots, t \ \text{ and } \ \sum_{k=0}^{t} a_{tk} = 1.$$

With this assumption the discrete dynamical system in (3) becomes a recurrence "with memory of the past"

$$p_{t+1} = F(p^{\mathrm{e}}_{t+1}), \quad p^{\mathrm{e}}_{t+1} = \sum_{k=0}^{t} a_{tk} p_k. \tag{8}$$

It is natural to assume (see, e.g. [35]) that recent prices are given higher weights than older ones. Thus, following [12,14,36], we shall assume weights which are exponentially decreasing as the terms of a geometric progression with memory ratio $\rho \in (0, 1)$:

$$a_{tk} = \frac{\rho^{t-k}}{W_t}, \qquad W_t = \sum_{k=0}^{t} \rho^{t-k}.$$

With these geometric weights, the expected prices are given by

$$p^{\mathrm{e}}_{t+1} = \sum_{k=0}^{t} \frac{\rho^{t-k}}{W_t} p_k \tag{9}$$

or, equivalently,

$$p^{\mathrm{e}}_{t+1} = \frac{W_t - 1}{W_t} p^{\mathrm{e}}_t + \frac{1}{W_t} p_t \tag{10}$$

which, by defining

$$\alpha_t = \frac{1}{W_t} \tag{11}$$

may be rewritten as

$$p^{\mathrm{e}}_{t+1} = (1 - \alpha_t) p^{\mathrm{e}}_t + \alpha_t p_t. \tag{12}$$

It shows that the expected prices are revised at each time period, in response to the forecasting error of the previous period, in a way similar to the mechanism of adaptive expectations proposed in (4), with the difference that the adjustment parameter $\alpha \in (0, 1)$, a constant there, is now replaced by a time-dependent speed of adjustment given by a decreasing sequence $\{\alpha_t\}$ with $\alpha_t \in (0, 1)$ for each t, and such that $\alpha_t \to (1 - \rho)$ as $t \to +\infty$. It is clear that by properly tuning the memory ratio ρ, different degrees of memory can be obtained: for small values of ρ, the memory of past prices vanishes very quickly and the limiting case $\rho \to 0$ reduces to static expectations. The other limiting value, $\rho \to 1$, describes the case in which all the previous prices are equally considered to compute the expected one. In order to compare this mechanism with the adaptive one in (4), we shall consider $\alpha = 1 - \rho$, i.e. $\rho = 1 - \alpha$, because we shall see that in this case the two different models are governed by the same one-dimensional "limiting map" given in (6).

If we replace p_t in (12) with its expression given in (3), we obtain a *non-autonomous* first-order difference equation (known in the literature as *Mann iteration* (see, e.g. [13,36])):

$$p^{\mathrm{e}}_{t+1} = (1 - \alpha_t) p^{\mathrm{e}}_t + \alpha_t F(p^{\mathrm{e}}_t). \tag{13}$$

In general, the study of the basins of attraction for the attractors of the recurrence (13) is not an easy task, since its limit sets are not invariant sets. However, taking into account that the partial sums of the geometric weights can be defined recursively as

$$W_t = 1 + \rho W_{t-1} \quad \text{for } t = 1, 2, \ldots; \quad W_0 = 1$$

or

$$\alpha_t = \frac{\alpha_{t-1}}{\alpha_{t-1} + \rho} \quad \text{for } t = 1, 2, \ldots; \quad \alpha_0 = 1$$

a two-dimensional *autonomous* system for $t \geq 1$ can be obtained from (13):

$$T_\alpha : \begin{cases} p^{\mathrm{e}}_{t+1} = (1 - \alpha_t) p^{\mathrm{e}}_t + \alpha_t F(p^{\mathrm{e}}_t) \\ \alpha_t = \dfrac{\alpha_{t-1}}{\alpha_{t-1} + \rho} \end{cases} \qquad \text{with i.c. } (p^{\mathrm{e}}_1, \alpha_0) = (p_0, 1). \tag{14}$$

The map T_α is equivalent to (13) because the projection on the p^{e} axis of any trajectory of (14) (i.e. any sequence of p^{e}_t values from that map) is also a solution of (13) associated with the same i.c. $\left(p^{\mathrm{e}}_1, \alpha_0\right) = (p_0, 1)$. Thus, the study of the non-autonomous recurrence (13) is reduced to the study of the two-dimensional map (14) with initial conditions only on the line $\alpha_0 = 1$. To rewrite the map as an

iterative process, we introduce $z = p^{\mathrm{e}}$ as in the previous section and obtain the following two-dimensional map:

$$T_{\alpha}: \begin{cases} z' = \dfrac{\rho}{\alpha+\rho} p_t^{\mathrm{e}} + \dfrac{\alpha}{\alpha+\rho} F(p_t^{\mathrm{e}}) \\ \alpha' = \dfrac{\alpha}{\alpha+\rho} \end{cases} \quad \text{with i.c. } (z_0, 1) = (p_1^{\mathrm{e}}, 1) = (p_0, 1) \tag{15}$$

and following [10], we also write the equivalent forms with different weights:

$$T_W: \begin{cases} p_{t+1}^{\mathrm{e}} = \left(1 - \dfrac{1}{W_t}\right) p_t^{\mathrm{e}} + \dfrac{1}{W_t} F(p_t^{\mathrm{e}}) \\ W_t = 1 + \rho W_{t-1} \end{cases} \quad \text{with i.c. } (p_1^{\mathrm{e}}, W_0) = (p_0, 1) \tag{16}$$

or

$$T_W: \begin{cases} z' = \dfrac{\rho W}{1+\rho W} z + \dfrac{1}{1+\rho W} F(z) \\ W' = 1 + \rho W \end{cases} \quad \text{with i.c. } (z_0, 1) = (p_1^{\mathrm{e}}, 1) = (p_0, 1). \tag{17}$$

Clearly, in the maps written above, we have to substitute $F(p_t^{\mathrm{e}})$ and $F(z)$ with the expression derived for the fishery model as described in Section 2, that is

$$F(z) = \frac{A - S_{\delta}(z)}{B}. \tag{18}$$

We remark again that even if the maps written above are two-dimensional, we are interested only in initial conditions belonging to the line $\alpha = 1$ or $W = 1$, called the *line of initial conditions*. However, as we shall see, the basins of attraction *must* be studied with two-dimensional techniques even if the attracting sets only depend on the one-dimensional *limiting map*

$$g_{1-\rho}(z) = \rho z + (1-\rho) F(z) \tag{19}$$

whose dynamics are completely known, and have been commented on the previous section (by writing $\alpha = (1-\rho)$). To see this, it is enough to consider the second equation of the two-dimensional maps, which are independent from z and describe two monotone sequences: one decreasing in α and converging to $\alpha^* = (1-\rho)$, the other increasing in W and converging to $W^* = 1/(1-\rho)$ (being partial sums of a geometric series of ratio ρ). The reason why we have maintained the double notation for the model with fading memory, by using the adjustment parameters as α_t or W_t is the following. Although the model written in (12) and (15) with α_t seems more suitable for an economic interpretation of the state, the dynamical properties (basins and their bifurcations) of that mathematical formulation are much more difficult to study. With the help of the second formulation in (10) and (17) with W_t, this difficulty is overcome and we can have a complete understanding of the fate associated with any given initial condition. This study will be done in the next section, in comparisons with the standard adaptive model, while in Section 4, we shall return to the other formulation and describe the dynamical difference in using the model with α_t.

3. Basins of the map T_W

In this section, we shall consider the dynamic model with statistical learning which reduces to the map T_W given in (17). The stability of the attractors of the model, all belonging to the line $W = W^*$ ($W^* = 1/(1-\rho)$), as noticed in the previous section, and their basins of attraction, can be studied on the basis of the following proposition stated in [12].

Proposition 2. *Let A be a k-cycle, $k \geq 1$, of the map $g_{1-\rho}(z)$, $0 \leq \rho \leq 1$. Then*

(i) *if A is attracting for the limiting map $g_{1-\rho}(z)$, then the set $\mathcal{A} = A \times \{W^*\}$ is an attracting cycle of the map T_W, and $F(A)$ is an attracting cycle of the model with statistical learning*;
(ii) *the basin of attraction B of the attractor $F(A)$ of the model with statistical learning is given by the intersection of the two-dimensional basin $\mathcal{B}$ of the cycle A of the map T_W with the line of initial conditions $W = 1$*;
(iii) *any invariant set of the map T_W must belong to $W = W^*$ (line of ω-limit sets) and is transversally attracting*.

We recall that the case $k = 1$ (cycle of period 1) corresponds to a fixed point z^* of $g(z)$, and $F(z^*) = z^*$ is a RE, since the fixed points of $g(z)$ are also fixed points of $F(z)$. From Proposition 1, we can deduce that the attractors of the recurrence (13), and their stability properties, are the same as those of the limiting map (19) and, moreover, we have the procedure to obtain the basins of attraction and their boundaries. This is particularly important when we have two coexisting attractors. In this case, the basin of attraction B of an attractor of the recurrence (13) is given by the intersection of the basin $\mathcal{B}$ of the corresponding attractor of T_W with the line of initial conditions:

$$B = \mathcal{B} \cap (W = 1).$$

To summarize, in the cases of multistability the knowledge of the exact structure of the basins of attraction is crucial. Such a knowledge cannot be obtained from the limiting map $g_{1-\rho}(z)$, because the initial conditions are to be taken on the line $W = 1$ whereas $g_{1-\rho}$ only governs the asymptotic dynamics on the line of ω-limit sets $W = W^*$. This means that only a global analysis of the two-dimensional map T_W allows us to follow the whole trajectory from the line of initial conditions to that of the ω-limit sets, thus taking into account the role of the short-run behavior, in which the dynamics are not governed by the limiting map $g_{1-\rho}$. Even if the trajectories of the map T_W starting from the line of initial conditions are entirely included in the strip of phase plane (z, W) with $W \in (1, W^*)$, we shall study the properties of the map T_W in the whole phase plane, because, in order to understand the properties of the basins, a global study of the action of the inverses is necessary. In fact, we first have to determine the basins of attraction of the two-dimensional map T_W, and this is obtained by considering the pre-images of a suitable neighborhood of the attracting sets located on the line of ω-limit sets. We recall that a closed invariant set $A \subset \{W = W^*\}$ is called asymptotically stable (or attracting) if a neighborhood U of A exists such that $T_W(U) \subseteq U$ and $T_W^n(z, W) \to A$ as $n \to +\infty$ for each $x \in U$. Then, the basin of attraction of A (a stable equilibrium or a more complex attracting set) is the open set of points which generate trajectories converging to A:

$$\mathcal{B}(A) = \{(z, W) : T_W^t(z, W) \to A \text{ as } t \to +\infty\}.$$

$\mathcal{B}(A)$ may be obtained by taking all the pre-images of the points in the neighborhood U

$$\mathcal{B}(A) = \cup_{n=0}^{\infty} T_W^{-n}(U),$$

where, in the case of a non-invertible map, $T_W^{-n}(x)$ denotes the set of all the pre-images of x of rank n, i.e. the set of all the points that are mapped into x after n applications of T_W. So, the study of the two-dimensional basins involves the inverses of. In this case, we have that the properties and the qualitative changes of its basins are strongly influenced by the presence of the denominator which can vanish along the line $W = -1/\rho$ and, in particular, by the points at which the first component of T_W has the form $0/0$. Some general properties of two-dimensional maps with a vanishing denominator have been studied in [37,38], and this particular class of triangular maps have been studied in [39]. In these papers, it is proved that the presence of points where a component of the map assumes the form $0/0$, called *focal points*, may have important consequences on the structure of the basins and their global bifurcations, because fans of basin boundaries arise from them giving peculiar finger-shaped structures called *lobes*.

The rational map T_W we are interested in is not defined on the whole plane, because the denominator of its first component vanishes for points belongings to the line $W = -1/\rho$, called the *singular line* of, and briefly denoted by δ_s. So, to have a well defined two-dimensional recurrence the singular line and all its pre-images of any rank must be excluded from the set of definition of T_W. By inverting the second component of T_W, we obtain $W = (W' - 1)/\rho$ from which we deduce that the points mapped by T_W onto the singular line δ_s are those belonging to the line δ_s^{-1} of equation $W = -(1 + \rho)/\rho^2$, which is below δ_s. In a similar way, we can also argue that the points which are mapped onto the singular line after n iterations of T_W are those on the line δ_s^{-n} of equation $W = -(1 - \rho^{n+1})/(\rho^{n+1} - \rho^{n+2})$, and these lines are all below δ_s, being $\delta_s^{-(n+1)}$ below δ_s^{-n} for all $n \geq 1$. Thus, the pre-images of any rank of δ_s belong to a sequence of lines located in the half plane $W < -1/\rho$ (out of interest for the application) and the domain of definition of T_W is given by $E = \mathbb{R}^2 \setminus \cup_{n=0}^{\infty} \delta_s^{-n}$.

Summarizing, the trajectories with initial conditions on the line $W = 1$ are entirely included in the region of the phase plane (z, W) with $W \in (1, W^*)$. The properties of the map T_W which are of interest in the economic context must be studied in the region $W \in (-1/\rho, W^*)$, because the basins' bifurcations start in that region (associated with the *singular line)*. Let us recall the following definition.

Definition. A point $Q = (x_Q, y_Q)$ is a focal point of a map T_W if at least one component of T_W assumes the form $0/0$ in Q and there exist smooth simple arcs $\gamma(t)$, with $\gamma(0) = Q$, such that $\lim_{\tau \to 0} T_W(\gamma(\tau))$ is finite. The set of all such finite values, obtained by taking different arcs $\gamma(t)$ through Q, is called the prefocal set δ_Q.

Roughly speaking, a prefocal curve is a set of points for which at least one inverse exists that maps (or focalizes) the whole set into a single point, called *focal point*.

For maps with a vanishing denominator, new kinds of contact bifurcations have been recently evidenced in [37,39]. These bifurcations involve the *singular line*, the *focal points* and the *prefocal set*. In particular, contacts between basin boundaries and prefocal curves may cause the creation of new kinds of structures of the basin boundaries denoted as *lobes*. The existence of lobes, issuing from the focal points, has important consequences on the structure of the basins of attraction of the model with learning whenever they intersect the line of initial conditions $W = 1$. This occurrence causes the creation of one dimensional basins with complicated topological structure, such as basins formed by many disjoint intervals, also with a chaotic structure.

As only the first equation of T_W has a denominator, which vanishes on the singular line $W = -1/\rho$, the focal points of T_W must necessarily belong to this line. On this line the numerator vanishes only for z such that $F(z) = z$, that is, for every fixed point of the function F which are also fixed points of the limiting map $g_{1-\rho}$. So, a focal point is always expressed by $(z^*, -1/\rho)$, where z^* is a fixed point of $F(z)$. This implies that the focal points of the map T_W are related to the existence of RE, since on all the points (z^*, W^*), where z^* is a fixed point of $F(z)$, the first component of T_W has the form $0/0$.

In order to evidence the role of a *focal point* and the related *prefocal set* in the dynamical behavior of the map T, we briefly describe here some geometric property (for more details we refer to [37,39]). The map T_W may be non-invertible, the number of distinct inverses of T_W depends on the structure of the function $F(z)$. In general, if $F(z)$ has N distinct fixed points, i.e. N distinct RE (and thus T_W also has N fixed points) then the prefocal line must belong to a region Z_N, whose points have N distinct rank-1 pre-images. The following proposition is proved in [39].

Proposition 3. *If $F(x)$ has N fixed points satisfying $F'(x^*) \neq 1$ then*

(i) *T_W has N focal points $Q_i = (z_i^*, -1/\rho)$ all associated with the same prefocal line δ_Q of equation $W = 0$;*
(ii) *the prefocal line of T_W belongs to a region Z_N where T_W has N distinct inverses;*
(iii) *for each focal point Q_i the map T_W defines a one-to-one correspondence between the slope m of an arc γ in Q_i and the point $(u, 0)$ in which the image $T_W(\gamma)$ crosses the prefocal curve δ_Q given by*

$$\begin{aligned} m \to (u,0): &\quad u = z_i^* + \frac{F'(z_i^*) - 1}{\rho m} \\ (u,0) \to m: &\quad m = \frac{F'(z_i^*) - 1}{\rho(u - z_i^*)} \end{aligned} \tag{20}$$

From the properties of the prefocal set, we can easily deduce the behavior of the rank-1 pre-images of a smooth arc η which intersects the prefocal line δ_Q at one point $(u, 0)$. Taking the arc η in the region Z_N (see the qualitative sketch in Fig. 6), then the N distinct rank-1 pre-images of η, say $T_{W,i}^{-1}(\eta)$, $i = 1, \ldots, N$, are arcs that intersect the singular line in the focal points $Q_i = (x_i^*, -1/\rho)$, with slope m_i as given in (20): $m_i(u) = (F'(x_i^*) - 1)/(\rho(u - x_i^*))$.

Some consequences of this correspondence, important for the characterization of the basin boundaries and their bifurcations, are deduced by considering a smooth arc η intersecting the prefocal line in two points, say $(u_1, 0)$ and $(u_2, 0)$, as shown Fig. 7, then each rank-1 pre-image of η, say $T_{W,i}^{-1}(\eta)$, has a loop with knot in the focal point $Q_i = (x_i^*, -1/\rho)$, and we have the following:

Proposition 4. *Let η be an arc which crosses the prefocal line in two points, say $(u_1, 0)$ and $(u_2, 0)$, and let $T_{W,i}^{-1}$ be an inverse of T_W which applies to all the points of η. Then each pre-image $T_{W,i}^{-1}(\eta)$ intersects the singular line at a focal point $Q_i = (z_i^*, -1/\rho)$ forming a loop with a double point in Q_i. The slopes of the two tangents in Q_i are given by $m_i(u_1)$ and $m_i(u_2)$ according to (20).*

From this proposition, we can easily deduce the kind of contact bifurcation that occurs when a smooth curve segment η moves toward the prefocal line δ_Q until a contact occurs followed by a crossing, as qualitatively shown in Fig. 8: as η moves toward δ_Q, its pre-images move towards Q_i, and when η

becomes tangent to δ_Q in the point $(u_c, 0)$ then each pre-image $\eta^i_{-1} = T^{-1}_{W,i}(\eta)$ has a cusp point in Q_i. The slope of the common tangent to the two arcs that join in Q_i is given by $m_i(u_c)$, according to (20). When the curve segment η crosses δ_Q at two points, say $(u_1, 0)$ and $(u_2, 0)$, then its pre-images gives loops with double points at the focal points Q_i.

Of course, when η is a portion of a basin boundary, a contact between η and δ_Q implies that a loop is created on the basin boundary, because a basin boundary includes all the pre-images of any portion of it, and the portion of the basin inside the loop is a lobe (see Fig. 8).

Now, let us consider the forward iteration of T_W. It is easy to see that the image of rank-n of the prefocal line $W = 0$ belongs to the line of equation $W = W_n$ where

$$W_n = \frac{1 - \rho^{n+1}}{1 - \rho} \tag{21}$$

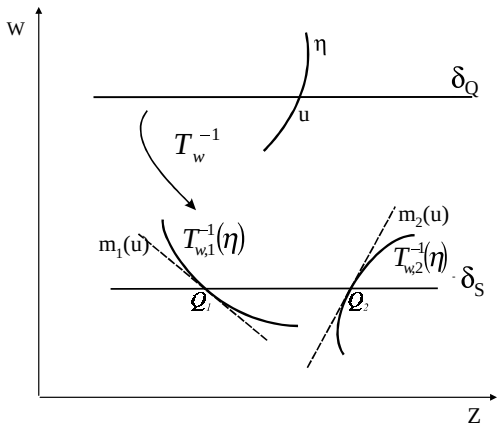

Fig. 6. Pre-images of an arc crossing the prefocal line at one point.

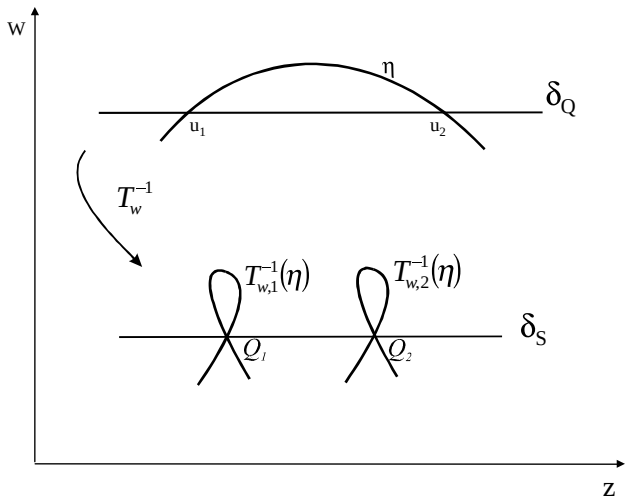

Fig. 7. Pre-images of an arc crossing the prefocal line at two points.

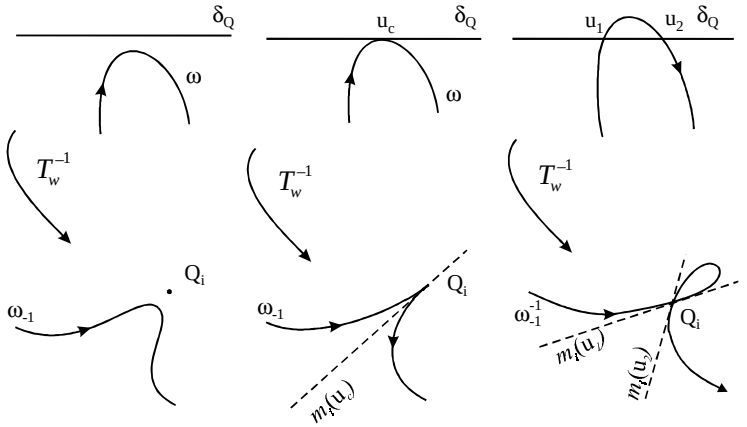

Fig. 8. Contact bifurcation with the prefocal set.

i.e. these images constitute a sequence of lines parallel to the prefocal line δ_Q and converging to the line of the ω-limit sets $W = W^*$. Thus, any cycle belonging to the ω-limit set $W = W^*$ is transversely attracting, and this property is important in order to study the boundaries of the basins. In fact, we recall that in general the boundaries of a basin are obtained by taking the stable sets of some cycle on it. In the case of maps T_W such cycles can only be of saddle type, and located on the line of ω-limit sets. To get the stable set W^s of a saddle it is enough to take the pre-images of any rank of a local stable set W^s_{loc}, that is $W^s = \cup_{n=0}^{\infty} T^{-n}(W^s_{loc})$, where W^s_{loc} is transverse to the line $W = W^*$ and its pre-images cannot have other cycles at finite distance as limit sets, since all the cycles of T_W belong to the line $W = W^*$. Thus, due to the expansive character of T_W^{-1} along the W direction, such pre-images must necessarily reach, in a finite number steps, the prefocal line $W = 0$. In this way, all these pre-images must necessarily cross the singular line $W = -1/\rho$ through focal points Q_i. From this observation, it follows that the stable set of any saddle cycle of T_W, obtained by taking the pre-images of a local stable set, is made up of branches issuing from the focal points, as stated in the following proposition:

Proposition 5. *All the branches of stable sets of all the saddle cycles of the map T_W are "focalized" through the focal points.*

From the arguments given above, it follows that if we consider an arc η, which intersects the line δ_Q at two points, then $T^{-1}_{W,i}(\eta)$ crosses the singular line at a focal point Q_i forming a loop. So. if we consider an arc η which intersects the line $W = W_j$, $j = 0, 1, \ldots, (n-1)$ at two points, then the set of the pre-images of rank n, $T_W^{-n}(\eta)$, can include N^n lobes issuing from the focal points $Q_1, \ldots, Q_N$. This behavior applied to the stable manifold of the saddle cycle (unstable RE) constitute the global mechanism causing the birth of particular structures which cause the difference between the adaptive model and the statistical one, as we shall see in the next section.

3.1. Basins in the fishery model

Up to now we have analyzed properties of the map T_W that hold whatever the function $F(z)$ is in its definition. In the following, we shall see the behavior of the map T_W when $F(z)$ is the function defined

in (18) and in Section 2. We are interested in comparing the model with statistical learning with the one with standard adaptive expectations considered in Section 2. Thus, let us consider the parameters given in (7), assuming $\rho = 1 - \alpha = 0.5$, so that we already know that for $0 < \delta < \delta_0$ the good equilibrium RE_3, and for $\delta_0 < \delta < \delta_1$, the good attractor A, are globally attracting for the limiting map. This is also true in the model with statistical learning, as no alternatives exist. So, except for a denumerable set of points (of zero Lebesgue measure), any i.c. $(z_0, 1)$ belongs to the basin of the attractor. Clearly, things change as the parameter δ increases. For $\delta > \delta_1$ on the line of ω-limit sets ($W^* = 1/(1-\rho)$), there are two coexisting stable attractors, RE_1 and A while $S^* = (s^*, W^*)$ is a saddle equilibrium whose stable set $W^s(S^*)$ separates the two basins of attraction, $\mathcal{B}(RE_1)$ and $\mathcal{B}(A)$. We know that for maps of this kind the vertical line through an equilibrium point belongs to its stable manifold, thus the local stable manifold of S^* is the line $z = s^*$, which we shall denote ω_0, and the global stable manifold of S^*, $W^S(S^*)$, is obtained by taking all the pre-images of any rank of ω_0:

$$W^S(S^*) = \bigcup_{n \geq 0} T_W^{-n}(\omega_0).$$

We can see the structure of this set directly in Fig. 9. On the line of ω-limit sets $W = W^*$ there are the equilibria S^* and RE_1, and the cycle A, and the picture shows the basins for the two-dimensional map T_W: the points in grey belong to the basin $\mathcal{B}(RE_1)$ while those in light grey belong to $\mathcal{B}(A)$ (those in dark grey will be explained below). Thus, the corresponding intervals on the line of ω-limit sets with $z > 0$ denote the basins of attraction of the two attractors under the standard adaptive mechanism, and are the same basins already commented in Section 2 (the basin of A is the interval $]s^*_{-1}, s^*[$ and the complementary set in $z > 0$ is the basin of RE_1 made up of two intervals), while the intersection with the line of initial

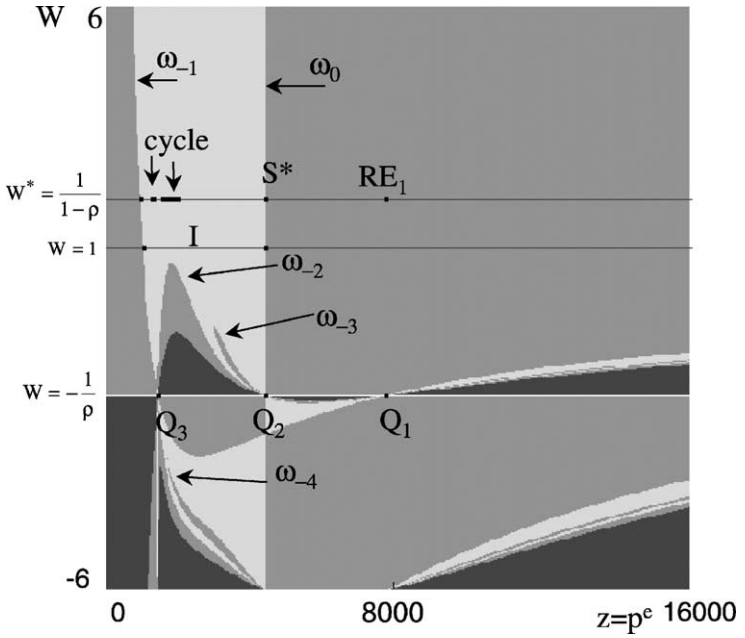

Fig. 9. Phase plane for the map T_W, the points in gray belong to the basin $\mathcal{B}(RE_1)$ while those in light grey belong to $\mathcal{B}(A)(\delta = 0.12)$.

conditions $W = 1$ gives the basins of attraction for the model with statistical learning. We can see in Fig. 9 that $B(A) = \mathcal{B}(A) \cap (W = 1)$ is still a connected interval, say I, $I =]s_l, s^*[$, which is slightly smaller than $]s^*_{-1}, s^*[$. This situation persists for values of δ in a (small) right interval of δ_1.

The structure of the stable set of S^* is influenced by the presence of the focal points of the map on the singular line δ_S, $W = -1/\rho$, mainly of Q_2 and Q_3. When $\delta > \delta_1$, there are three focal points located on the intersection between the singular line δ_S and the vertical line through the equilibrium points. The stable set of S^* is clearly observable in Fig. 9, being the boundary separating the two basins of attraction (i.e. the frontier between the points in grey and those in light grey): the local stable manifold, the vertical line ω_0, $z = s^*$, crosses the focal point Q_2 associated with the fixed point S^*, the rank-1pre-image is denoted by ω_{-1}, and is a curve which crosses the focal point Q_3 associated with the stable equilibrium RE_3, the pre-image of rank-2 of ω_0 includes a curve denoted by ω_{-2} which crosses the focal points Q_2, Q_3 and Q_1, the pre-image of rank-3 includes a curve denoted by ω_{-3} which crosses the focal points Q_2, Q_3, and a curve denoted by ω_{-4} which approaches the focal point from below, and so on. Let us first remark how the existence of the focal points (although in a region out of interest in the applied model) causes global bifurcations in the structure of the basins which lead to different trajectories and different asymptotic behavior associated with the same i.c. in the two different kinds of learning mechanism here considered. For low values of δ, as it is the case represented in Fig. 9, there are not many differences between the basins of attraction $B(A)$ in the two models (with adaptive expectations and with statistical ones), and similarly for $B(\mathrm{RE}_1)$. However, we can see in Fig. 9 that the arc ω_{-2} has crossed the prefocal line $W = 0$, let us say at the bifurcation value δ_{c_0} ($\delta_{c_0} \simeq 0.09$), and is approaching the region of interest, i.e. the line of initial conditions $W = 1$, as δ increases. When ω_{-2} has a contact with (and then intersects) the prefocal line $W = 0$, at δ_{c_0}, two branches of ω_{-3} have a cusp at the focal points Q_2 and Q_3 and then cross the focal points creating lobes of the basin $\mathcal{B}(\mathrm{RE}_1)$, as can be seen in Fig. 9, and when ω_{-2} has a contact with the line $W = 1$, say at the bifurcation value δ_{c_1}, the two lobes bounded by ω_{-3} have a contact with the prefocal line $W = 0$ and ω_{-4} has cusp points at the focal points (see Figs. 10 and 11), preparing the creation of four new lobes issuing from Q_2 and Q_3 for $\delta > \delta_{c_1}$.

It is clear that δ_{c_1} denotes the first contact bifurcation for the model with statistical expectations, as the contact between the boundary $\partial\mathcal{B}(\mathrm{RE}_1)$ and the line of initial conditions $W = 1$ (via the arc ω_{-2}), changes the basin $B(A)$ because for $\delta > \delta_{c_1}$ the basin $B(A)$ is no longer an interval but it will be the union of two intervals (for δ not far from δ_{c_1}):

$$B(A) = \mathcal{B}(A) \cap \{W = 1\} = I_1 \cup I_2.$$

The two intervals are separated by a portion of the basin of the other equilibrium, $B(RE_1) = \mathcal{B}(RE_1) \cap \{W = 1\}$, as shown in Fig. 10. We can equivalently say that in the previous interval I a "hole" of points belonging to the other basin $B(\mathrm{RE}_1)$ has been created at this first contact bifurcation. From Fig. 11, we can also see that the second contact bifurcations between the boundary $\partial\mathcal{B}(\mathrm{RE}_1)$ and the line of initial conditions $W = 1$ (via the two arcs of ω_{-3}), just occurred, say at $\delta = \delta_{c_2}$, at which value four, 2^2, arcs bounded by ω_{-4} have a contact with the prefocal set $W = 0$ and 2^3 arcs bounded by ω_{-5} are issuing from the focal points creating new lobes. For $\delta > \delta_{c_2}$, the basin $B(A)$ is no longer made up of two intervals as it will be the union of four intervals (for δ not far from δ_{c_2}), or, equivalently we can say that two more "holes" of the basin $B(\mathrm{RE}_1)$ will appear in the old interval I. And so on: a very fast sequence of contact bifurcations occurs as δ increases, causing the transition of the basin $B(A)$ from the union of 2^n intervals to the union of 2^{n+1} much smaller intervals, and increasing, in number and in size, the "holes" of the basin $B(\mathrm{RE}_1)$ inside the old interval I.

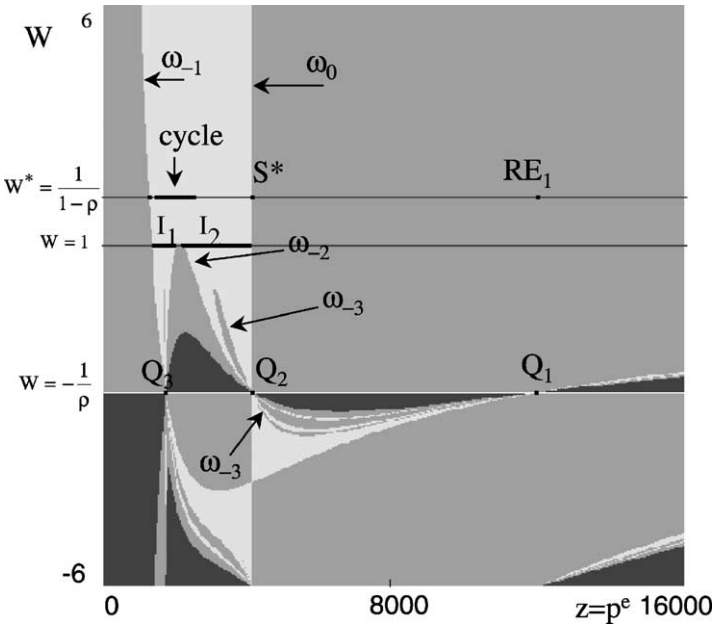

Fig. 10. Map T_W. First contact bifurcation for the basins ($\delta = 0.18$).

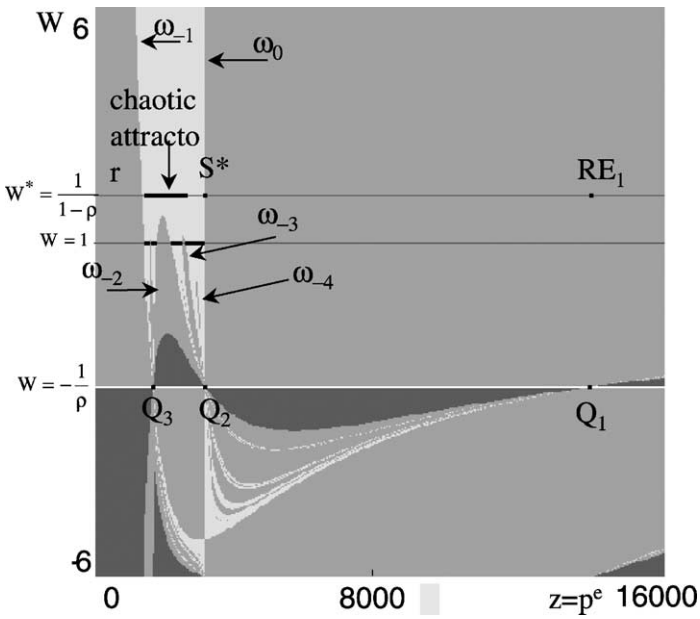

Fig. 11. Map T_W. Second contact bifurcation for the basins ($\delta = 0.9$).

As we have already noticed, on the line $W = W^*$, the basin of the equilibrium A is always the connected interval $]s^*_{-1}, s^*[$. Thus, we can conclude that different dynamics occur with the two different mechanisms for the expected values, as whenever we take an i.c. $z = z_0$ in one of the "holes" of the old interval I, we shall obtain a sequence of states converging to the good attractor A in the case of adaptive mechanism, while with a more sophisticated learning mechanisms the states will converge to the bad equilibrium RE_1.

Moreover, this is not the only difference of behavior between the two mechanisms. In fact, as we have remarked in Section 2, the model with standard adaptive expectations is always "well posed" in the positive axis $z > 0$, as by iterating the map $g_\alpha(z)$ any i.c. with $z_0 > 0$ will give a sequence of positive values which is convergent somewhere, either to the bad equilibrium RE_1 or to some different attracting set in the bounded interval $]s^*_{-1}, s^*[$ (and this can be observed also on the line of ω-limit sets $W = W^*$). This is no longer the case in the model with statistical learning. In the figures of this section there is also a dark grey region which we have not yet commented on. The vertical axis $z = 0$ separates points of the half plane $z < 0$ from those having $z > 0$ so that the pre-images of any rank of this line separate points which belong to the basin $\mathcal{B}(\mathrm{RE}_1)$ from those having at least one state in the region $z < 0$, and that we shall call *unfeasible*. That is: the dark grey points denote *unfeasible* states, as any point belonging to the dark grey region has a trajectory with a state in the half plane $z < 0$, reached in a finite number of steps.

It is worth noting that for the values of the parameter δ considered in the previous figures the unfeasible region is unimportant for the economic model because that region has no contacts with the line of initial conditions $W = 1$, but we may expect that as δ increases there will be a contact, followed by a crossing, between the dark grey region and the line of initial conditions we are interested in. In fact, the boundary of the dark grey region is obtained from the pre-images of any order of the line $z = 0$, and also these pre-images follow the usual rules of the inverses of such kinds of maps, and are influenced by the existence of the focal points. Whenever an arc crosses the prefocal line $W = 0$ in two points, then its pre-images issue from the focal points creating lobes, and when this occurs to the boundary of the dark grey region we get lobes belonging to the unfeasible region. As δ increases the arcs move toward higher values of W, so that it is reasonable to have crossing also of the line $W = 1$.

We end this section by noticing the remarkable differences between the adaptive mechanism and the statistical one, as for a wide interval of values of the parameter δ the basin B of the low-level attractor A is disconnected and may also have a fractal structure, and for many initial conditions $z_0 \in]s^*_{-1}, s^*[$ (which may also be the widest part) the model with geometric memory converges toward RE_1, and there exist, i.c. also very close to A, which may have non-admissible trajectories.

4. Dynamics and basins of the map T_α

From an economic point of view it would be of interest to study directly the dynamic behavior of the model with geometric memory as given in (14) (or in (15)), because the adaptive parameters α_t, which change in time, are susceptible of an economic interpretation. Clearly, taking into account that $\alpha_t = 1/W_t$, in this section, we are not giving new results, because the sequences α_t can easily be deduced from the W_t. However, we shall describe the study of the map in (15) because it is quite different from the study performed in the previous section, and it gives us the opportunity to show how the bifurcations in two-dimensional non-invertible maps may occur via contacts at infinity, on the Poincaré equator (PE henceforth).

Thus, in this section we consider the two-dimensional map in (15), which we rewrite for convenience:

$$T_\alpha : \begin{cases} z' = \dfrac{\rho}{\alpha+\rho} p_t^{\mathrm{e}} + \dfrac{\alpha}{\alpha+\rho} F(p_t^{\mathrm{e}}) \\ \alpha' = \dfrac{\alpha}{\alpha+\rho} \end{cases} \qquad \text{with i.c. } (z_0, 1) = (p_1^{\mathrm{e}}, 1) = (p_0, 1). \tag{22}$$

The map T_α is not defined on the whole plane because the denominators of both components vanish on the line δ_{S} of equation

$$\delta_{\mathrm{S}} : \qquad \alpha = -\rho \tag{23}$$

so that T_α is well defined only if we exclude the singular line from the phase plane as well as its pre-images of any rank. The pre-images of δ_{S} belong to a sequence of lines located above δ_{S}, that is, in the strip $-\rho < \alpha < 0$. In fact, it is easy to invert the second component of T_α obtaining

$$\alpha = \frac{\alpha'\rho}{1-\alpha'}$$

from which we have that the points mapped by T_α on the singular line δ_{S} in one iteration are the points of the line $\delta_{\mathrm{S}}^{-1}$of equation

$$\delta_{\mathrm{S}}^{-1} : \quad \alpha = -\frac{\rho^2}{1+\rho} \tag{24}$$

which is located above δ_{S}, and so on, the points mapped on the singular line after n iterations of T_α belong to the line δ_{S}^{-n} of equation

$$\delta_{\mathrm{S}}^{-n} : \quad \alpha = \frac{-\rho^{n+1}}{\sum_{k=0}^{n} \rho^k} = -\frac{\rho^{n+1} - \rho^{n+2}}{1-\rho^{n+1}}. \tag{25}$$

We remark that all these lines are located above δ_{S}, as the line $\delta_{\mathrm{S}}^{-(n+1)}$ is higher than δ_{S}^{-n} for $n \geq 1$ and have the line $\alpha = 0$ as the accumulation set when $n \to +\infty$. Thus, the domain of definition of the map T_α is given by $E = \Re^2 \setminus \cup_{n=0}^{\infty} \delta_{\mathrm{S}}^{-n}$.

We already know that the second component of T_α gives rise, starting from $\alpha_0 = 1$, to a decreasing sequence of α_t values converging to $\alpha^* = 1 - \rho$ as $t \to \infty$, so that the limiting map of T_α is the one-dimensional map $z' = g_{1-\rho}(z)$ located on the line $\alpha = \alpha^*$, called the line of ω-limit sets.

As the map T_α has a vanishing denominator in the points of the line $\alpha = -\rho$, it follows that focal points must necessarily belong to it. On $\alpha = -\rho$ the numerator of the first component of T_α becomes $\rho[z - F(z)]$, thus it vanishes if and only if $F(z) = z$, that is, at each fixed point of the function F and also of the limiting map. It follows that the first component of T_α takes the form $0/0$ in the points $Q = (z^*, -\rho)$, where z^* is a fixed point of $F(z)$ (and thus a RE). In our model, considering that $F(z)$ is the function defined in (18), we have that for $\delta > \delta_1$ three points of this kind exist, denoted by Q_1, Q_2 and Q_3, associated with the equilibria RE_1, S^* and RE_3, respectively, and it is immediate to see that such points are particular focal points of T_α, due to the fact that both the functions defining T_α have a vanishing denominator. In fact, although the first component of T_α has finite limiting values, on different arcs which cross these points, the second component of T_α is always divergent. Thus, the values that usually constitute the prefocal set in the map T_α, are now at infinity and thus belong to the PE. However, a one-to-one correspondence can be

established between the slopes of arcs through Q and the points on the PE (which recalls the one existing for the focal points, given in (20) for maps having only one function with a vanishing denominator). To see this, let us consider an arc γ transverse to δ_S in a point $Q = (z^*, -\rho)$, represented in parametric form by

$$\gamma(\tau) : \begin{cases} z(\tau) = z^* + \xi_1\tau + \xi_2\tau^2 + \cdots \\ W(\tau) = -\rho + \eta_1\tau + \eta_2\tau^2 + \cdots \end{cases} \qquad \tau \neq 0. \tag{26}$$

To study the shape of the set $T_\alpha(\gamma)$, let us assume that γ is deprived of the point $(z^*, -\rho)$, so that the arc can be considered as the union of two disjoint pieces, say $\gamma = \gamma_+ \cup \gamma_-$, where γ_- and γ_+ are obtained from (26) with $\tau < 0$ and $\tau > 0$, respectively. Considering the image $T_\alpha(\gamma)$ we have

$$\lim_{\tau\to 0\pm} T(\gamma(\tau)) = \left(z^* + \rho\frac{\xi_1}{\eta_1}[F'(z^*) - 1], \mp\infty\right) \tag{27}$$

thus $T_\alpha(\gamma)$ is made up of two unbounded arcs, located on opposite side of the phase plane, issuing from the point (27) of the PE. Let $m = \eta_1/\xi_1$ be the slope of the tangent to the arc γ in the point $(z^*, -\rho)$, we may write

$$\lim_{\tau\to 0\pm} T(\gamma(\tau)) = (u_m, \mp\infty), \quad \text{with} \quad u_m = z^* + \rho\frac{F'(z^*) - 1}{m}. \tag{28}$$

As m varies in $\Re\backslash\{0\}$ we obtain all the points of the PE. Thus, we may extend the definition given in [37,39] and quoted in Section 3, for maps having only one function with a vanishing denominator, to maps in which both the functions have a vanishing denominator. The points Q_i are particular focal points of T_α, as all the arcs crossing Q_i with slope m are mapped by T_α in two unbounded arcs which are transverse to the PE in the point $(u_m, \mp\infty)$, where u_m is given in (28) with the suitable value of z^*, and the prefocal set does not assume finite value, being the PE. And we already know that the points Q_i assume a particular importance in the explanation of the bifurcations occurring in the basins of attraction. Moreover, also the points at infinity, that is on the PE, are endowed with properties similar to those of the prefocal line of the maps T_W. In fact, the pre-images of an arc crossing the PE give loops issuing from the focal points, and thus lobes in the basins.

We now describe the sequence of bifurcations concerning the basins of attraction of the map T_α, considering the same cases of the previous section (that is, $\rho = 0.5$ and increasing δ), considering the figures giving the basins of the two coexisting RE for $\delta > \delta_1$. In Fig. 12, the equilibria are evidenced on the line of ω-limit sets $\alpha = \alpha^* = 1 - \rho$, the basin $\mathcal{B}(\mathrm{RE}_1)$ is made up of grey points while the basin $\mathcal{B}(A)$ is the one in light grey and, as in the previous section, the dark grey points denote the unfeasible set of i.c. whose trajectories enter the half-plane $z < 0$ (and the frontier is made up of the pre-images of any rank of $z = 0$).

The intersection of the basins with the line $\alpha^* = 1 - \rho$ gives the basins for the model with standard adaptive expectations, and we already know that the basin of A is the interval $]s^*_{-1}, s^*[$. The intersection of the basins with the line of initial conditions $\alpha = 1$ gives the basins for the model T_α with statistical expectations, and we already know that the basin of A, for δ close to δ_1, is an interval smaller then $]s^*_{-1}, s^*[$. The stable set of the saddle S^* gives the boundary of the basins of the two equilibria, and the local stable manifold is always the line $z = s^*$ denoted by ω_0, crossing the singular line in the focal point Q_2, and we can see that the rank-1pre-image includes an arc ω_{-1} crossing the focal point Q_3, the rank-2 pre-image

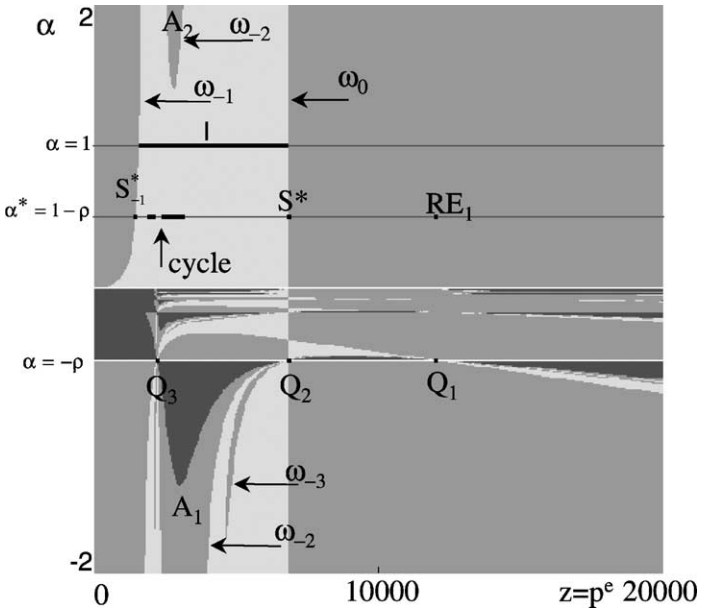

Fig. 12. Phase plane of the map $T_\alpha(\delta = 0.12)$.

includes an arc ω_{-2} which issues from the focal points Q_3 and Q_2, bounding a portion of basin $\mathcal{B}(A)$ denoted A_1 in Fig. 12. As δ increases, this portion A_1 increases going down towards $-\infty$ of the z-axis and the contact with infinity, i.e. the contact with the PE occurs at the bifurcation value δ_{c_0} at which two arcs of ω_{-3} have cusps in the focal points preparing the creation of two lobes issuing from them. For $\delta > \delta_{c_0}$, the portion A_1 crosses the PE creating a new area coming from above ($+\infty$ of the z-axis) and denoted by A_2 in Fig. 12, and at the same time the two lobes bounded by ω_{-3} are going down towards $-\infty$ of the z-axis, and the contact with the PE occurs at the bifurcation value δ_{c1}, at the same time 2^2 arcs of ω_{-4} have cusps in the focal points preparing the creation of four new lobes issuing from them. At $\delta = \delta_{c1}$ the first bifurcation of the basins occurs because the portion A_2 of the basin $\mathcal{B}(\mathrm{RE}_1)$ reaches (from above) the line of initial conditions $\alpha = 1$ (see Fig. 13).

For $\delta > \delta_{c_1}$, the basin we are interested in becomes disjoint, $B(A) = \mathcal{B}(A) \cap \{\alpha = 1\} = I_1 \cup I_2$, that is, in the previous interval I a "hole" of points belonging to the other basin $B(\mathrm{RE}_1)$ has been created at this first contact bifurcation. For $\delta > \delta_{c_1}$, the two lobes bounded by ω_{-3} cross the PE giving rise to two new lobes coming from above ($+\infty$ of the z-axis), reaching the line of initial conditions at $\delta = \delta_{c_2}$ (see Fig. 14), and at the same time the 2^2 arcs of ω_{-4} (going down towards $-\infty$ of the z-axis) have a contact with the PE and 2^3 arcs of ω_{-5} have cusps in the focal points preparing the creation of eight new lobes issuing from them. For $\delta > \delta_{c_2}$, the basin $B(A)$ is made up of 2^2 disjoint smaller intervals, that is, in the previous interval I three "holes" of points belonging to the other basin $B(\mathrm{RE}_1)$ have been created. And so on, infinitely many contact bifurcations occur with the PE (and thus with the line of initial conditions), modifying at each contact the structure of the basins for the model with statistical learning.

We end this section observing that we can clearly describe the contact bifurcations with the PE due to our knowledge of the properties of the map T_W, and the results observed in this model with the map T_α are important not only for the economic interpretation of the model (which can be obtained also in

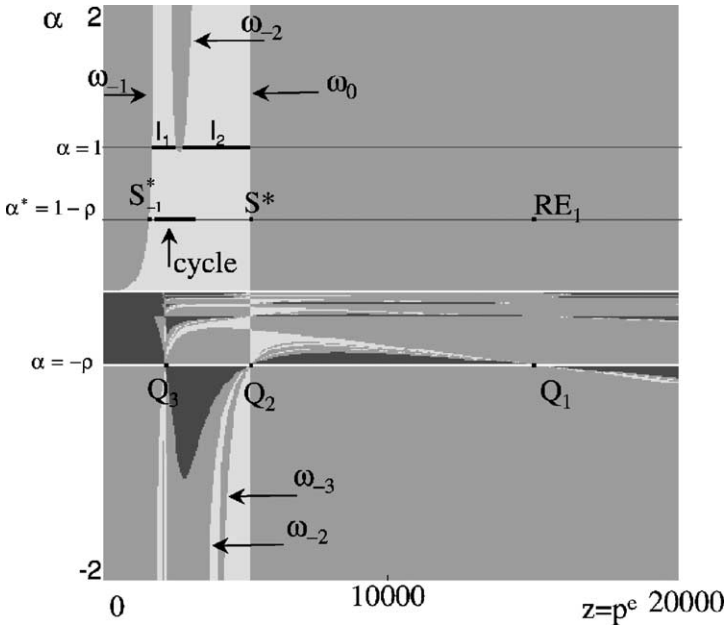

Fig. 13. Map T_α. First contact bifurcation for the basins ($\delta = 0.18$).

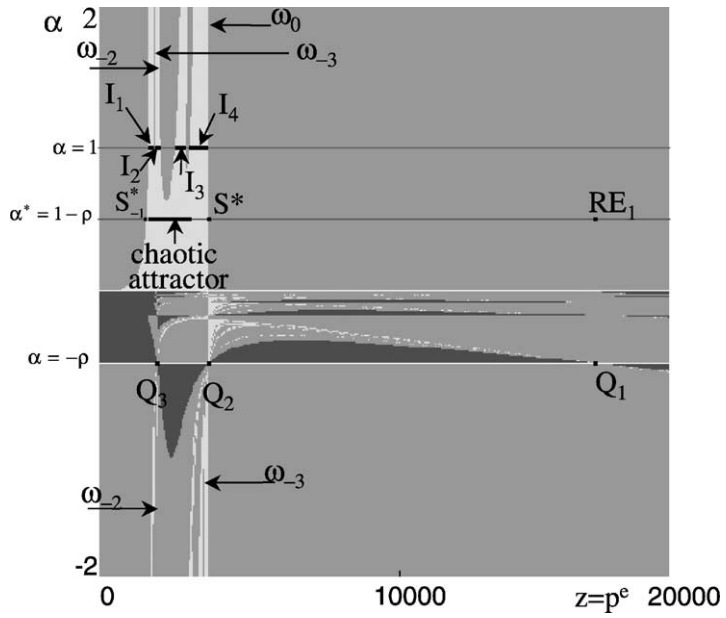

Fig. 14. Map T_α. Second contact bifurcation for the basins ($\delta = 0.9$).

Section 3) but also for the mathematical properties of the particular focal points, associated with prefocal sets at infinity, on the PE, due to maps having both the functions with a vanishing denominator.

5. Conclusion

We extended the analysis of the model of renewable resource markets developed by Hommes and Rosser [9] by comparing its simple adaptive expectations learning mechanism with a geometrically declining statistical learning mechanism. Our analysis considered the global properties of the respective mechanisms and found considerable differences as the discount rate rises above a critical level where more complex dynamics are observed in the original model. The statistical learning model is associated with much more complicated patterns of basin boundaries of the coexisting attractors. These complications include the emergence of zones of unfeasible points as well as the appearance of lobes on the basin boundaries that imply holes in one basin containing points of another basin. The complexity of this phenomenon is much enhanced for the case of particular focal points associated with prefocal sets at infinity, that is in the Poincaré equator.

This difference between the two learning mechanisms suggests that in the face of complex dynamics it may be safer for agents to fall back on simpler adaptive mechanisms than to follow more sophisticated learning systems that make use of more information. Such a conclusion echoes an argument made previously by Heiner [40] that agents tend to rely on simple rules of thumb as complexity increases and that this can be a stabilizing strategy. Arguably this is also implicit in the findings of Hommes and Rosser, and earlier of Hommes [41], that agents may be able to learn to believe in chaotic dynamics using relatively simple adaptive mechanisms.

Acknowledgements

This work has been performed under the activity of the national research project "Non-linear Models in Economics and Finance: Complex Dynamics, Disequilibrium and Strategic Interactions", MIUR, Italy.

Appendix A. The fishery model

In this appendix, we recall, for the sake of completeness, the model proposed in [9]. The Gordon–Schaefer fishery model of a population growth and harvesting is based on a differential equation of the form

$$\frac{\mathrm{d}x}{\mathrm{d}t} = f(x) - h(t)$$

where $x(t)$ denotes the size of the resource population at time t (t is expressed in days), $f(x)$ is a given function representing the natural growth rate of the population and h_t represents the rate of removal or harvesting [28–30] it is assumed

$$f(x) = rx\left(1 - \frac{x}{k}\right). \tag{A.1}$$

where the constant r, assumed to be positive, is called *intrinsic growth rate*. The positive constant k is usually referred to as the environmental *carrying capacity* or saturation level. If $f(x) = h(t)$ the fish population remains at a constant level or, in other words, the natural growth rate $f(x)$ equals the sustainable yield that can be harvested without changing the fixed level population x. In case of constant harvesting, that is when $h(t) = h$, the condition of sustainable harvesting of renewable resources becomes

$$h = rx\left(1 - \frac{x}{k}\right). \tag{A.2}$$

We remark that, for the population level $x = (k/2)$, there exists a *maximum sustainable yield* (MSY)

$$h_{\mathrm{MSY}} = \max f(x)$$

with the property that any larger harvest rate will lead to the depletion of the population. The level $x = (k/2)$ can be considered optimal from a biological point of view but we have to notice that the cost of catching fish tends to rise as the population is reduced. When the costs as well as the benefits are taken into consideration, it might be argued that the optimal stock level should be higher than $k/2$. In this assumption, the *catch-per-unit-effort* is proportional to the stock level, that is

$$h = qEx$$

where E denotes fishing effort and q is the catchability coefficient. So the equilibrium harvest, or sustainable yield $Y = h$ corresponding to E is given by

$$Y = qEx.$$

If p represents the price of the fish per unit, the total revenue will be

$$R(Y) = pY = pqEx \tag{A.3}$$

whereas the total cost is given by

$$C(E) = cE \tag{A.4}$$

with c the constant marginal cost of effort E.

It is assumed that the sole owner's objective is the maximization of the total discounted net revenues derived from the exploitation of the resource. If $\delta > 0$ is a constant denoting the rate of discount and $c[x(t)]$ equals the unit harvesting cost when the population level is x, this objective may be expressed as

$$\max_{h(t)} \int_0^{+\infty} \mathrm{e}^{-\delta t}(p - c[x(t)])h(t)\,\mathrm{d}t. \tag{A.5}$$

Solving (A.5) subject to the conditions $x(t) \geqslant 0$ and $h(t) \geqslant 0$ is an optimal control problem. As $\dot{x} = \mathrm{d}x/\mathrm{d}t = f(x) - h(t)$, substituting $h(t) = f(x) - \dot{x}$ into (A.5)

$$\max_{h(t)} \int_0^{+\infty} \mathrm{e}^{-\delta t}(p - c[x(t)])(f(x) - \dot{x})\,\mathrm{d}t. \tag{A.6}$$

is obtained. Applying the Euler necessary condition for a maximum to solve (A.6), we get:

$$f'(x) - \frac{c'(x)\,f(x)}{p - c(x)} = \delta. \tag{A.7}$$

We remark that (A.7) is an implicit equation for the population x. The solution $x = x^*$ of (A.7) is the optimal equilibrium population level. For the model in [29] it is

$$c(x) = \frac{c}{qx}, \qquad f(x) = rx\left(1 - \frac{x}{k}\right)$$

and

$$c'(x) = -\frac{c}{qx^2}, \qquad f'(x) = r - \frac{2rx}{k} \tag{A.8}$$

Substituting (A.8) into (A.7), a quadratic equation in x is get, with positive solution

$$x^*_\delta(p) = \frac{k}{4}\left\{1 + \frac{c}{pqk} - \frac{\delta}{r} + \sqrt{\left(1 + \frac{c}{pqk} - \frac{\delta}{r}\right)^2 + \frac{8c\delta}{pqkr}}\right\}. \tag{A.9}$$

The sustained yield corresponding to (A.9) is given by $Y = f(x^*_\delta(p))$ and the market supply curve is

$$S_\delta(p) = h = f(x^*_\delta(p)). \tag{A.10}$$

References

[1] R.E. Lucas, T.J. Sargent (Eds.), Rational Expectations and Econometric Practice, vol. I, University of Minnesota Press, Minneapolis.
[2] T.J. Sargent, Bounded Rationality in Macroeconomics, Clarendon Press, Oxford, 1993.
[3] T.J. Sargent, The Conquest of American Inflation, Princeton University Press, Princeton, 1998.
[4] O.J. Blanchard, Output, the stock market and interest rates, Am. Econ. Rev. 71 (1981) 132–143.
[5] R. Thaler, The Winner's Curse: Paradoxes and Anomalies of Economic Life, Free Press, New York, 1992.
[6] J. Conlisk, Why bounded rationality? J. Econ. Liter. 34 (1996) 669–700.
[7] R. Marimon, Learning from learning in economics, in: D.M. Kreps, K.F. Wallis (Eds.), Advances in Economics and Econometrics: Theory and Applications, vol. I, Cambridge University Press, Cambridge, UK, 1997.
[8] G.W. Evans, S. Honkapohja, Increasing social returns, learning and bifurcation phenomena, in: A. Kirman, P. Salmon (Eds.), Learning and Rationality in Economics, Basil Blackwell, Oxford, 1995, pp. 216–235.
[9] C.H. Hommes, J.B. Rosser Jr., Consistent expectations equilibria and complex dynamics in renewable resource markets, Macroecon. Dyn. 5 (2001) 180–203.
[10] G.I. Bischi, L. Gardini, Equilibrium selection and transient dynamics under adaptive and statistical learning, Working Paper No. 9, Diploma di Economia, Università di Parma, 2000.
[11] R.E. Lucas, Adaptive behavior and economic theory, J. Business 59 (4) 1986.
[12] G.I. Bischi, L. Gardini, Mann iterations reducible to plane endomorphisms, No. 36, Quaderni di Economia, Matematica e Statistica, Facoltà di Economia, Università di Urbino, 1996.
[13] G.I. Bischi, A. Naimzada, L. Gardini, Infinite distributed memory in discrete dynamical systems, No. 39, Quaderni di Economia, Matematica e Statistica, Università di Urbino, 1996.
[14] G.I. Bischi, A. Naimzada, Global analysis of a non-linear model with learning, Econ. Notes 26 (3) (1997) 143–174.
[15] I. Foroni, Meccanismi di apprendimento in modelli omogenei ed eterogenei, Ph.D. Thesis, University of Trieste, 2001.
[16] C. Chiarella, Perfect foresight models and the dynamic instability problem from a higher viewpoint, Econ. Modell. 4 (1986) 283–292.
[17] C. Chiarella, The bifurcation of probability distributions in a non-linear rational expectations model of a monetary economy, Eur. J. Pol. Econ. 7 (1991) 65–78.
[18] C. Chiarella, The dynamics of speculative behavior, Ann. Oper. Res. 37 (1991) 101–123.
[19] C.H. Hommes, Adaptive learning and roads to chaos: the case of the cobweb, Econ. Lett. 36 (1991) 127–132.

[20] C.H. Hommes, On the consistency of backward-looking expectations: the case of the cobweb, J. Econ. Behav. Organ. 33 (1998) 333–362.
[21] P. Flashel, R. Sethi, The stability of models of monetary growth: implications of non-linearity, Econ. Modell. 2 (1999) 307–316.
[22] G.I. Bischi, R. Marimon, Global stability of inflation target policies with adaptive agents, Macroecon. Dyn. 5 (2) (2001) 148–179.
[23] A. Agliari, D. Delli Gatti, M. Gallegati, L. Gardini, Global dynamics in a non-linear model for the equity ratio, Soliton Fractals 11 (2000a) 961–985.
[24] A. Agliari, L. Gardini, T. Puu, The dynamics of a triopoly Cournot game, Solitons Fractals 11 (2000b) 2531–2560.
[25] G.I. Bischi, M. Kopel, Equilibrium selection in a non-linear duopoly game with adaptive expectations, J. Econ. Behav. Organ. 46 (2002) 73–100.
[26] J.B. Rosser Jr., From Catastrophe to Chaos, A General Theory of Economic Discontinuities, Kluwer Academic Publishers, Boston, 1991.
[27] J.B. Rosser Jr., Complex ecologic–economic dynamics and environmental policy, Ecol. Econ. 37 (2001) 23–37.
[28] H.S. Gordon, The economic theory of a common-property resource: the fishery, J. Pol. Econ. 62 (1954) 124–142.
[29] M.B. Schaefer, Some considerations of population dynamics and economics in relation to the management of marine fisheries, J. Fisher. Res. Board Can. 14 (1957) 669–681.
[30] C.W. Clark, Mathematical Bioeconomics: The Optimal Management of Renewable Resources, second ed., Wiley/Interscience, New York, 1990.
[31] P. Copes, The backward-bending supply curve of the fishing industry, Scottish J. Pol. Econ. 17 (1970) 69–77.
[32] J.E. Conklin, W.C. Kolberg, Chaos for the halibut? Mar. Resour. Econ. 9 (1994) 153-182.
[33] C. Mira, L. Gardini, A. Barugola, J.C. Cathala, Chaotic Dynamics in Two-Dimensional Non-invertible Maps, Non-linear Sciences, Series A, World Scientific, Singapore, 1996.
[34] C. Mira, Chaotic Dynamics, World Scientific, Singapore, 1987.
[35] B.M. Friedman, Optimal expectations and the extreme information assumption of rational expectations macromodels, J. Monet. Econ. 5 (1979) 23–41.
[36] F. Aicardi, S. Invernizzi, Memory effects in discrete dynamical systems, Int. J. Bifurc. Chaos 2 (4) (1992) 815–830.
[37] G.I. Bischi, L. Gardini, C. Mira, Maps with denominator. Part I. Some generic properties, Int. J. Bifurc. Chaos 9 (1) (1999) 119–153.
[38] G.I. Bischi, L. Gardini, C. Mira, Plane maps with denominator. Part II. Some bifurcation cases, Int. J. Bifurc. Chaos, in press.
[39] G.I. Bischi, L. Gardini, Basin fractalization due to focal points in a class of triangular maps, Int. J. Bifurc. Chaos 7 (7) (1997) 1555–1577.
[40] R.A. Heiner, The origin of predictable dynamic behavior, J. Econ. Behav. Organ. 12 (1989) 221–232.
[41] C.H. Hommes, G. Sorger, Consistent expectations equilibria, Macroecon. Dyn. 2 (1998) 287–321.